JOURNAL OF MATERIALS SCIENCE 31 (1996) 5027–5031

Response of aluminium/graphite composite to deformation in the semi-solid state

C. P. CHEN, C.-Y.A. TSAO
Department of Materials Science and Engineering, National Cheng Kung University, Tainan, Taiwan

Semi-solid deformation of Al/graphite (Gr) composites was studied. The effects of deformation temperatures and deformation rates on the macrostructures, morphologies, the deformation force, and the formability of the composites were studied. For Al–10 wt % Gr composites, the semi-solid deformation stress increases as strain increases at lower strain rate. At higher strain rate, the stress first increases to a local maximum, then decreases before it starts to increase again as strain increases. For Al–30 wt % Gr composites, the stress decreases as strain increases. For both the Al–10 wt % Gr composites and Al–30 wt % Gr composites, the higher the deformation strain rate is, the more severe is the degree of cracking. The higher the deformation strain rate, the larger is the deformation stress, not counting the effects of fracturing. The deformation stresses required to semi-solid-deform Al–30 wt % Gr composites are larger than those for Al–10 wt % Gr composites, which is contrary to the normal solid-state deformation behaviours of Al–Gr composites. Composites deformed at 620 °C tend to require a higher deformation stress than at 630 °C for the same deformation strain, due to smaller liquid fraction and lower ductility at 620 °C. The effects of deformation temperatures on the ductility of the compacts are not significant at lower deformation strain rate. However, at the highest deformation strain rate, the ductility is better for higher deformation temperature.

1. Introduction

The study on the behaviour of metals in the semi-solid state was pioneered by Spencer at MIT in 1971 [1]. He applied a shear strain on solidifying Sn–15%–Pb alloy, and discovered a remarkable reduction in shear stress compared with those that were not sheared during solidification. The grain structure of the sheared alloy was non-dendritic, as opposed to the dendritic structure of not-sheared alloy. Since this early work, semi-solid processing (SSP), including semi-solid synthesizing (SSS) and semi-solid forming (SSF), has become a widely studied and accepted process. Semi-solid forming is a process combining elements of both casting and forging and is an effective net-shape forming process [2–4]. Compared with conventional cast materials, SSP materials have less segregation and finer grain size. Practically, SSP can increase part-forming rate, reduce the thermal shock imposed on the mould, increase mould life and reduce the force applied during forming, etc. [1–16].

Metal–matrix composites (MMCs) possess many advantages over monolithic materials, e.g. higher specific strength, good wear resistance, higher thermal conductivity than ceramic materials, lower coefficient of thermal expansion, etc., and have been used in the aircraft, space, defence and automotive industries [17–20]. One of the most common processes for manufacturing MMCs is the powder metallurgy process (P/M) [21]. However, a complete P/M process may be elaborate and more costly.

The objectives of this study were to combine the P/M and the SSF processes into an integrated net-shape forming process. 6061 Al powder and graphite powder were mixed and cold-pressed into compacts, which were then heated to the desired temperatures in the semi-solid regime and deformed. In the experiment, the effects of the Gr wt % and the temperatures and deformation strain rates of the deformation on the macrostructures, morphologies, and the deformation behaviours of the composites were studied.

2. Experimental methods

Mixtures of 6061 Al powder (average powder size: 30 mm) and Gr powder (average powder size: 30 mm) of two weight ratios, 10 wt % and 30 wt % of Gr, were mixed in a V-shape mixer for 12 h at 100 r.p.m. The mixtures were then cold-pressed using a 50.8 t hydraulic press into cylindrical compacts of Al/Gr MMC preforms. The dimensions of the compacts were 12 mm in diameter × 12 mm in length. The compacts were then semi-solid-deformed directly.

Semi-solid forming was performed with a 10.16 t Instron machine, model 1125. The compacts were placed between graphite plates, through which

0022–2461

TABLE I Process parameters of semi-solid deformation

Sample No.	Composite compositions	Deformation temperature (°C)	Initial strain rate (s^{-1})
5	Al–10 wt % Gr	620	0.00083
7	Al–10 wt % Gr	620	0.0083
6	Al–10 wt % Gr	620	0.083
4	Al–10 wt % Gr	630	0.00083
2	Al–10 wt % Gr	630	0.0083
13	Al–10 wt % Gr	630	0.083
22	Al–30 wt % Gr	620	0.00083
28	Al–30 wt % Gr	620	0.0083
21	Al–30 wt % Gr	620	0.083
34	Al–30 wt % Gr	630	0.00083
32	Al–30 wt % Gr	630	0.0083
38	Al–30 wt % Gr	630	0.083

thermocouples were inserted to contact the compacts directly from the top and the bottom. A three-zone temperature-controlled furnace was used to control the temperature of the compacts with the feedbacks from the thermocouples. The differences in temperatures between top and bottom of the compacts were controlled to be within $\pm 2.5\,^{\circ}C$.

Two semi-solid deformation temperatures were chosen to study the effects of the deformation temperatures, which were 620 and 630 °C, both were in the liquid-plus-solid two-phase regime of 6061 Al. The compacts were heated to the set temperature for semi-solid deformation, then held for 10 min to equalize the temperatures within the compacts before the onset of semi-solid deformation. Three deformation speeds, 0.6, 6 and 60 mm min^{-1}, corresponding to initial deformation strain rates of 8.3×10^{-4}, 8.3×10^{-3} and $8.3 \times 10^{-2}\,s^{-1}$, respectively, were used to study the effects of the deformation rates. Table I lists the experimental parameters used for the composite samples. The compacts were deformed from 12 to 6 mm high, corresponding to a true deformation strain of -0.69. The compacts were quenched immediately after the deformation was finished to preserve the as-deformed macrostructures of the compacts. The force versus displacement relationships were recorded.

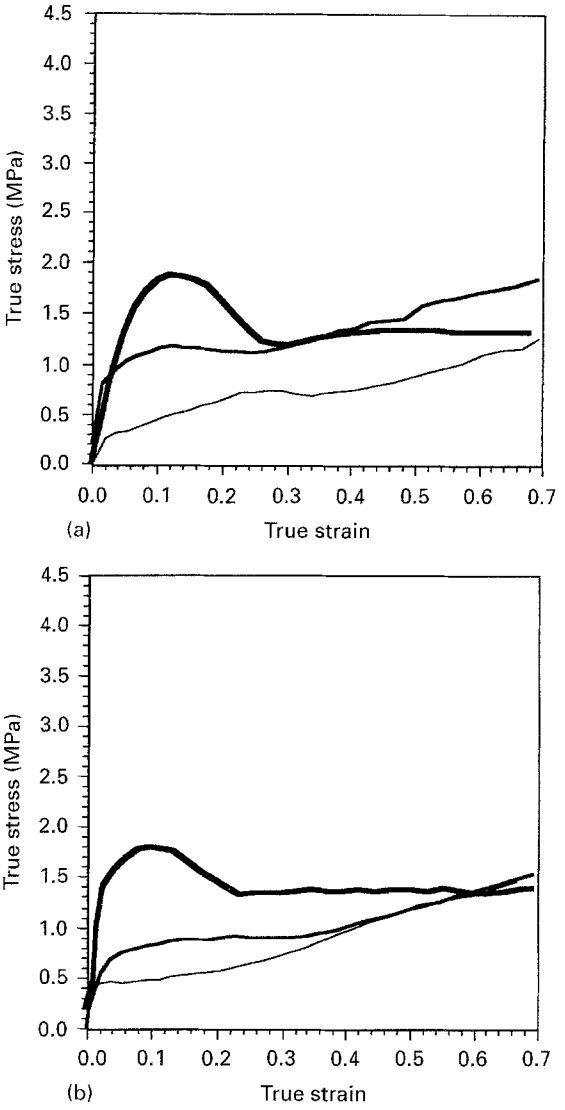

Figure 1 Variations of deformation stress with deformation strain for Al–10 wt % Gr composites at various deformation strain rates at deformation temperature of (a) 620 °C; (b) 630 °C. — 0.00083 s^{-1}; — 0.0083 s^{-1}; — 0.083 s^{-1}.

3. Results and discussion

Figs 1 and 2 show the effects of deformation strain rates on the deformation stress versus strain relationships of the semi-solid deformation for various Gr wt % and deformation temperatures. The behaviours of Al–10 wt % Gr composites at different deformation temperatures are consistent, as shown in Fig. 1. At the highest deformation strain rate, $8.3 \times 10^{-2}\,s^{-1}$, the deformation stress first increases to a local maximum, then decreases before it starts to increase again as deformation strain increases for both 620 and 630 °C deformation temperatures. This can be explained by observing the morphologies of the composites, as shown in Figs 3 and 4 for Al–10 wt % Gr composites deformed at 620 and 630 °C, respectively. The morphologies of the composites can be distinguished by two portions, a central round disc, and an outer ring where ductility was exhausted and fracturing appeared, which is a common appearance to all compressed materials. The small holes shown at the centre of each compact are the indentation marks from the thermocouples, from which some liquid phase was shown to be squeezed out. It is shown that as the deformation strain rate increases, the fracture in the outer ring becomes more severe. It is because that the time for the composites to flow plastically was less at higher deformation strain rate, so the composites did not have enough time to flow plastically, resulting in limited ductility. At the highest deformation strain rate, the outer ring started to fracture into pieces, which resulted in a decrease of the deformation stress in the initial deformation stage. However, the central round disc shows no fracture at all, which kept the deformation stress at a constant level in the later deformation stage. At lower deformation strain rates, $8.3 \times 10^{-3}\,s^{-1}$ and $8.3 \times 10^{-4}\,s^{-1}$, the deformation stress increases as deformation strain increases all the time, since the fracture was not severe enough that at

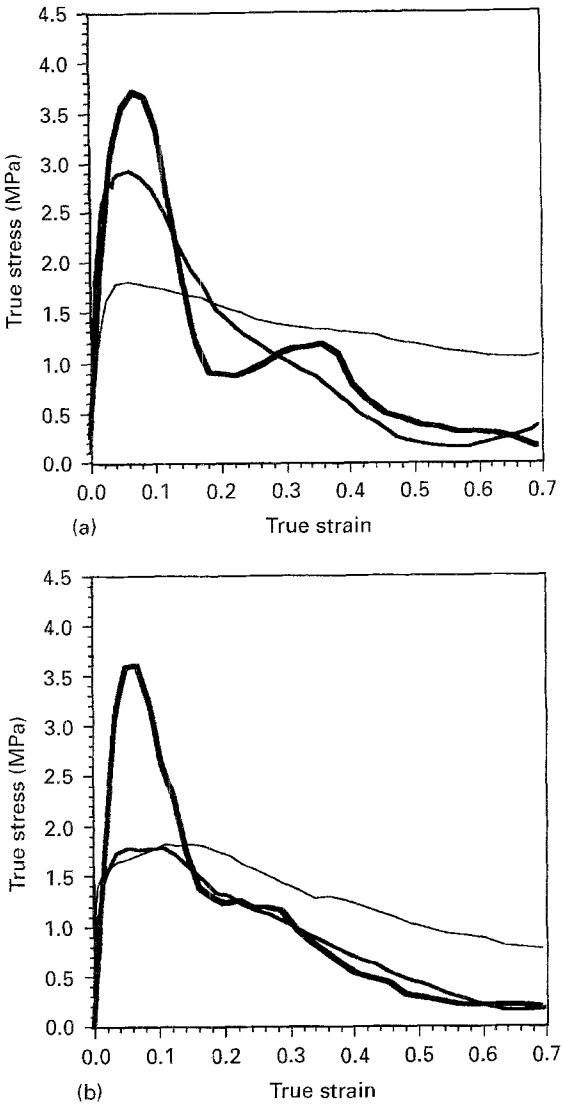

Figure 2 Variations of deformation stress with deformation strain for Al–30 wt % Gr composites at various deformation strain rates at deformation temperature of (a) 620 °C; (b) 630 °C. See Fig. 1 for key.

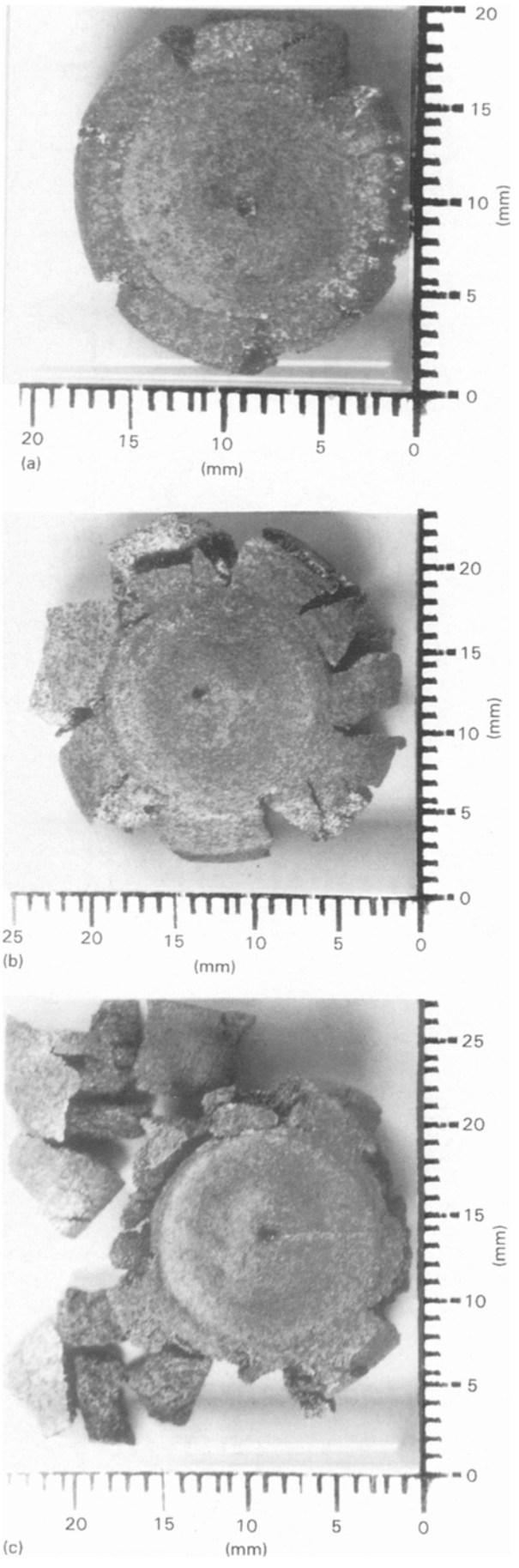

Figure 3 Morphologies of Al–10 wt % Gr composites after semi-solid deformation at 620 °C at a strain rate of (a) $8.3 \times 10^{-4}\,s^{-1}$; (b) $8.3 \times 10^{-3}\,s^{-1}$, and (c) $8.3 \times 10^{-2}\,s^{-1}$, (top view).

the highest deformation strain rate to cause the deformation stress to decrease. It is shown that the greater the deformation strain rate, the larger the deformation stress is required, not counting the effects of the severe fracture occurring at the highest deformation strain rate.

As for the Al–30 wt % Gr composites, the deformation stress versus strain behaviours, as shown in Fig. 2, are completely different from those of Al–10 wt % Gr composites. The deformation stress decreases as deformation strain increases continuously, which can also be explained by observing the morphologies of the composites shown in Fig. 5 for Al–30 wt % Gr composites deformed at 620 °C. All the Al–30 wt % Gr composites fracture severely, which show not only a fractured outer ring, but fractured central discs, except the composite deformed at the lowest deformation strain rate, in which the central disc shows no severe fracturing. As a result, the deformation stress decreases all the time as deformation strain increases, for all the Al–30 wt % Gr composites. The double maximum deformation stresses shown for both the

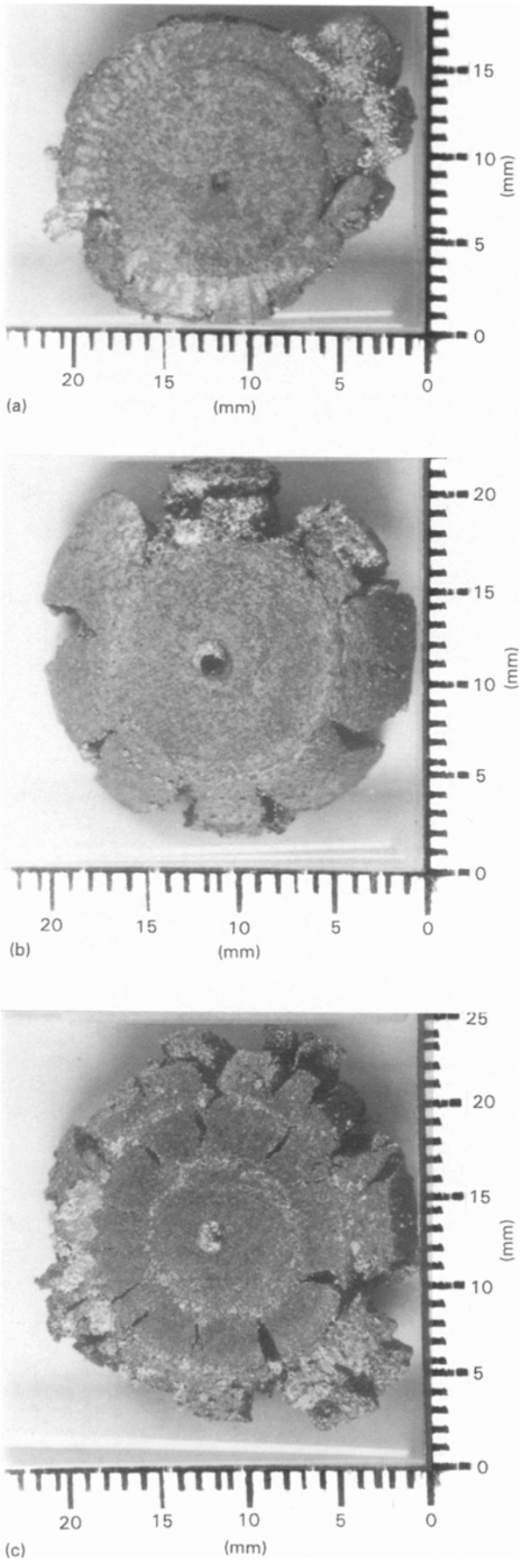

Figure 4 Morphologies of Al–10 wt % Gr composites after semi-solid deformation at 630 °C at strain rate of (a) $8.3 \times 10^{-4}\,s^{-1}$; (b) $8.3 \times 10^{-3}\,s^{-1}$, and (c) $8.3 \times 10^{-2}\,s^{-1}$, (top view).

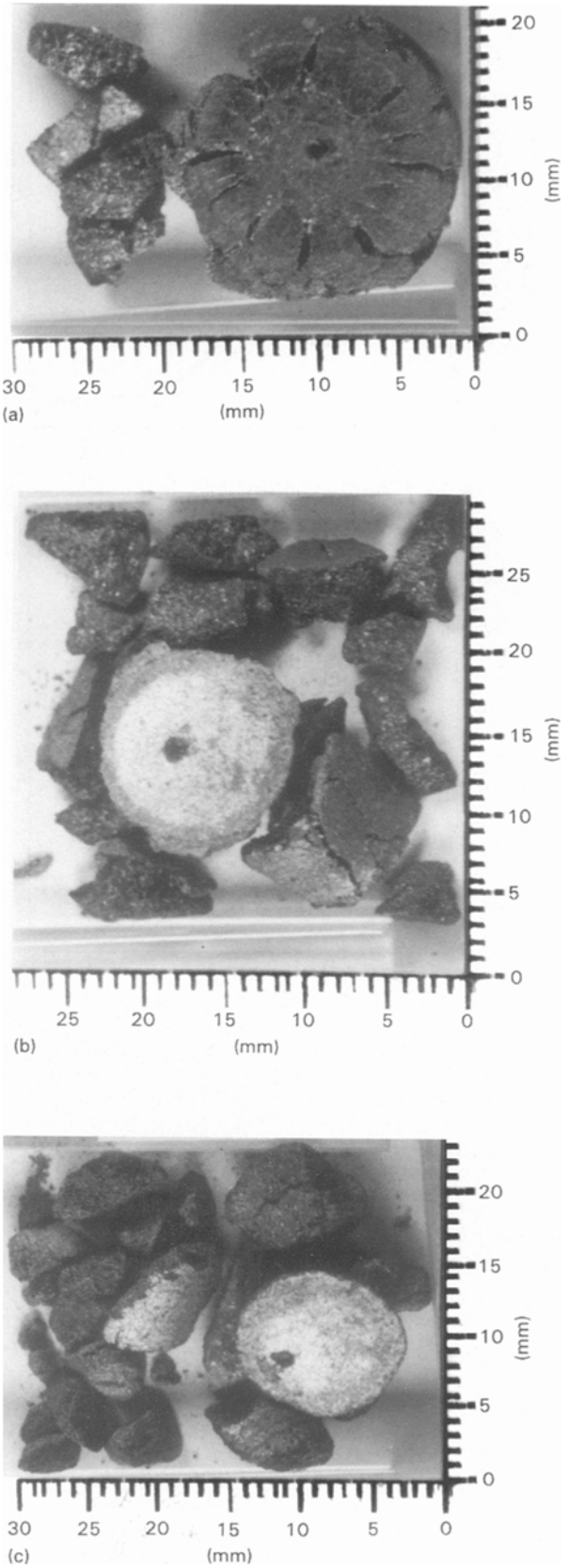

Figure 5 Morphologies of Al–30 wt % Gr composites after semi-solid deformation at 620 °C at a strain rate of (a) $8.3 \times 10^{-4}\,s^{-1}$; (b) $8.3 \times 10^{-3}\,s^{-1}$, and (c) $8.3 \times 10^{-2}\,s^{-1}$, (top view).

composites deformed at the highest strain rate, $8.3 \times 10^{-2}\,s^{-1}$, were probably the result of complicated cracking events occurring during the deformation. It is also shown that the higher the deformation strain rate, the larger the deformation stress is required not counting the effects of fracturing.

The effects of Gr wt % on the deformation stress versus strain relationships of the semi-solid deformation are shown by comparing Fig. 1 with Fig. 2. In normal deformation in the fully solid state, the deformation stress required to deform Al–Gr composites decreases as graphite content increases, since aluminium is stronger than graphite, the addition of which resulted in the decrease of overall composite strength. However, in the present study, the initial deformation stresses required to semi-solid-deform Al–30 wt % Gr composites are larger than those required for Al–10 wt % Gr composites for all the deformation strain rates and temperatures studied. This is because since the graphite was in solid form at the semi-solid deformation temperatures applied in the present study, the larger the graphite content, the smaller was the liquid fraction presenting in the composites, at a specific semi-solid deformation temperature. Consequently, the overall strength of the Al–30 wt % Gr composites, due to their lower solid fraction, were higher than that of the Al–10 wt % Gr composites, which means that the deformation stress required to deform Al–30 wt % Gr composites was larger than that required to deform Al–10 wt % Gr composites. As for the deformation stress at larger deformation strain, the comparison would be meaningless since Al–30 wt % Gr composites started to fracture at greater deformation strain.

The effects of deformation temperatures on the deformation stress versus strain relationships of the semi-solid deformation are shown in Figs 1 and 2, separately. There are no significant differences in deformation stresses between the composites deformed at 620 and 630 °C for all the deformation strain rates and Gr wt % studied. However, composites deformed at 620 °C tend to require higher deformation stresses than those deformed at 630 °C for the same deformation strain, which was due to smaller liquid fraction and lower ductility at 620 than at 630 °C. The effects of deformation temperatures on the morphologies of the compacts are not significant at lower deformation strain rates (i.e. 8.3×10^{-4} and $8.3 \times 10^{-3} s^{-1}$) as shown by comparing Fig. 3 with Fig. 4 for 620 and 630 °C, respectively. However, at the highest deformation strain rate (i.e. $8.3 \times 10^{-2} s^{-1}$) the Al–10 wt % Gr composites show severe outer ring fracturing into pieces at 620 °C, while they show less fracturing at 630 °C; this indicates that the ductility is better at higher deformation temperature.

4. Conclusions

1. For Al–10 wt % Gr composites, the semi-solid deformation stress increases as strain increases at lower strain rate. At higher strain rate, the stress first increases to a local maximum, then decreases before it starts to increase again as strain increases. For Al–30 wt % Gr composites, the stress decreases as strain increases.
2. For both the Al–10 wt % Gr composites and Al–30 wt % Gr composites, the higher the deformation strain rate, the more severe is the degree of cracking.
3. The higher the deformation strain rate, the larger is the deformation stress, not counting the effects of fracturing.
4. The deformation stresses required to semi-solid-deform Al–30 wt % Gr composites are larger than those for Al–10 wt % Gr composites, which is contrary to the normal solid-state deformation behaviours of Al–Gr composites.
5. Composites deformed at 620 °C tend to require a higher deformation stress than at 630 °C, for the same deformation strain, due to smaller liquid fraction and lower ductility at 620 °C.
6. The effects of deformation temperatures on the ductility of the compacts are not significant at lower deformation strain rate. However, at the highest deformation strain rate, the ductility is better for higher deformation temperature.

Acknowledgement

Support from the National Science Council under grant no. NSC 82-0405-E-006-411 is gratefully acknowledged.

References

1. D. B. SPENCER, R. MEHRABIAN and M. C. FLEMINGS, *Metall. Trans.* **3** (1972) 1925.
2. M. C. FLEMINGS, *Ibid.* **22A** (1991) 957.
3. D. H. KIRKWOOD and P. KAPRANOS, *Casting Technology*, **Jan.** (1986) 16.
4. S. B. BROWN and M. C. FLEMINGS, *Adv. Mater. Proc.* **Jan.** (1993) 36.
5. J. F. SECONDE and M. SUERY, *J. Mater. Sci.* **19** (1984) 3995.
6. V. LAXMANN and M. C. FLEMINGS, *Metall. Trans. A* **11A** (1980) 1927.
7. M. SUERY and M. C. FLEMINGS, *Ibid.* **13A** (1982) 1809.
8. Y. S. YANG and C. -Y. A. TSAO, *Scripta Metall. Mater.* **30** (1994) 1541.
9. C. P. CHEN and C. -Y. A. TSAO, in Proceedings of 1994 PM^{2}TEC'94 Conference, MPIF-APMI, Toronto, Canada, 1994.
10. H. LEHUY, J. BLAIN, G. L. BATA and J. MASOUNAVE, *Metall. Trans. B* **15B** (1984) 173.
11. P. KAPRANOS, D. H. KIRKWOOD and C. M. SELLAR, *Proc. Inst. Mech. Engrs* **207B** (1993) 1.
12. M. A. TAHA and M. SUERY, *Metals Tech.* **11** (1984) 226.
13. P. O. CHARREYRON and M. C. FLEMINGS, *Int. J. Mech. Sci.* **27** (1985) 781.
14. L. A. LALLI, *Metall. Trans. A* **16A** (1985) 1393.
15. M. KIUCHI and S. SUGIYAMA, *J. Mater. Shaping Tech.* **8** (1990) 39.
16. K. MIIWA, K. KOBAYASHI and T. NISHIO, in Proceedings of the 3rd International Conference on Semi-Solid Processing of Alloys and Composites (1994) p. 483.
17. P. NISKANEN and W. R. MOHN, *Adv. Mater. Proc. Aug.* (1988) 39.
18. M. HUNT, *Mech. Eng.* **July** (1989) 43.
19. L. KEMPFER, *Ibid.* **Aug.** (1990) 19.
20. M. HUNT, *Ibid.* **June** (1990) 27.
21. M. K. JAIN, V. V. BHANU PRASAD, S. V. KAMAT, A. B. PAANDEY, V. A. VARMA, B. V. R. BHAT and Y. R. MAHAIAN, *Int. J. Powd. Metall.* **29** (1993) 267.

Received 8 December 1995
and accepted 13 February 1996